Oral administration of Huanglian-Houpo herbal nanoemulsion loading multiple phytochemicals for ulcerative colitis therapy in mice

Xiao Wang, Li Fu, Weijian Cheng, Jiamei Chen, Huan Zhang, Huanjun Zhu, Chen Zhang, Chaomei Fu, Yichen Hu & Jinming Zhang

Taylor & Francis
Taylor & Francis Group

RESEARCH ARTICLE

Oral administration of Huanglian-Houpo herbal nanoemulsion loading multiple phytochemicals for ulcerative colitis therapy in mice

Xiao Wang[a], Li Fu[a], Weijian Cheng[a], Jiamei Chen[a], Huan Zhang[a], Huanjun Zhu[a], Chen Zhang[a], Chaomei Fu[a], Yichen Hu[b] and Jinming Zhang[a]

[a]State Key Laboratory of Southwestern Chinese Medicine Resources, Pharmacy School, Chengdu University of Traditional Chinese Medicine, Chengdu, China; [b]Key Laboratory of Coarse Cereal Processing of Ministry of Agriculture and Rural Affairs, Chengdu University, Chengdu, China

ABSTRACT

How to achieve stable co-delivery of multiple phytochemicals is a common problem. This study focuses on the development, optimization and characterization of Huanglian-HouPo extract nanoemulsion (HLHPEN), with multiple components co-delivery, to enhance the anti-ulcerative colitis (UC) effects. The formulation of HLHPEN was optimized by pseudo-ternary phase diagram combined with Box-Behnken design. The physicochemical properties of HLHPEN were characterized, and its anti-UC activity was evaluated in DSS-induced UC mice model. Based on preparation process optimization, the herbal nanoemulsion HLHPEN was obtained, with the droplet size, PDI value, encapsulation efficiency (EE) for 6 phytochemicals (berberine, epiberberine, coptisine, bamatine, magnolol and honokiol) of 65.21 ± 0.82 nm, 0.182 ± 0.016, and $90.71 \pm 0.21\%$, respectively. The TEM morphology of HLHPEN shows the nearly spheroidal shape of particles. The optimized HLHPEN showed a brownish yellow milky single-phase and optimal physical stability at 25 °C for 90 days. HLHPEN exhibited the good particle stability and gradual release of phytochemicals in SGF and SIF, to resist the destruction of simulated stomach and small intestine environment. Importantly, the oral administration of HLHPEN significantly restored the shrunk colon tissue length and reduced body weight, ameliorated DAI value and colon histological pathology, decreased the levels of inflammatory factors in DSS-induced UC mice model. These results demonstrated that HLHPEN had a significant therapeutic effect on DSS-induced UC mice, as a potential alternative UC therapeutic agent.

Abbreviations: UC: ulcerative colitis; 5-ASA: 5-aminosalicylic acid; HLHPEN: nanoemulsion of Huanglian-HouPo extract; PDI: polydispersity index; EE: encapsulation efficiency; LE: loading efficiency; TEM: transmission electron microscopy; O/W: Oil-in-water; W/O: water-in-oil; DSS: Dextran sulfate Sodium; DAI: Disease activity index; IL 6: Interleukin 6; IL 1β: Interleukin 1β; TNF-α: Tumor necrosis factor α; IL 10, Interleukin 10

Introduction

Ulcerative colitis (UC), as a chronic and refractory colon disease, brings huge physiological harm and economic burden to patients (Kobayashi et al., 2020; Shi et al., 2020). These currently first-line drugs, such as 5-aminosalicylic acid (5-ASA), corticosteroids, immunosuppressants, etc., usually suffer the limited efficacy and obvious side effects. The previous pre-clinical and clinical studies have demonstrated that Traditional Chinese Medicine (TCM) as well as these plant-derived bioactive compounds would be an important breakthrough point, with the effective UC treatment effect and high biosafety (He et al., 2022; Liu Y et al., 2022). Huanglian-Houpo (HLHP) formula, consisting of *Coptidis Rhizoma* (Huanglian in Chinese, HL) and *Magnolia officinalis Cortex* (Houpo in Chinese, HP), is a TCM classic formula recorded in TCM Classics "*Prescriptions for Universal Relief (Puji Fang)*" in 15th century AD (Zhang FL et al., 2022). HLHP formula has been used for hundreds of years to treat gastrointestinal diseases such as abdominal pain, diarrhea and bloody stool, which were similar to the clinical symptoms of

UC. Likewise, Wang et al have demonstrated that HL-HP herb pair could significantly suppress UC in a TNBS-induced rats by protecting the intestinal barrier and regulating the intestinal flora (Xie Q et al., 2022).

In our previous study, the fraction of HLHP extracted by 50% ethanol exhibited the higher anti-UC effects than HLHP decoction. However, as well-known, there are multiple chemical components in HL-HP combination, in which the hydrophobic components like magnolol and honokiol, and the hydrophilic components like berberine and epiberberine, exhibited the recognized anti-UC effects (Shen et al., 2018; Li C et al., 2020; Jing et al., 2021). Interestingly, these compounds manifested the different benefits in UC treatment, as well as the different water solubility, oral bioavailability and pharmacokinetic behaviors. For example, berberine, a hydrophilic representative component of HL, has an excellent anti-UC effect mediated by a variety of mechanisms, such as modulating enteric glial cells-intestinal epithelial cells-immune cells interactions, regulating colonic intestinal flora, and regulating several inflammation-associated signaling pathways (Jing et al., 2021). However, berberine has insufficient druggability, because it is easy to combine with baicalin, glycyrrhizic acid, baicalin and other components to form a poorly water-soluble conjugate, which makes it difficult for its intestinal malabsorption to play its role (Okoshi et al., 2021; Zhang S et al., 2022). Nevertheless, the benefits of magnolol for UC would accelerate colonic mucosal barrier repair and prevent the mucosal damage, but it has the limitation of low oral bioavailability (Zhao et al., 2017). Meanwhile, even magnolol and honokiol, these two natural compounds with similar chemical structure, also exhibit different physicochemical and stability properties (Usach et al., 2021). Therefore, the colon-specific delivery system loaded with multiple components is still urgently needed for these bioactive phytochemicals in HL-HP combination.

Although the nano- or micro-sized vehicles based on natural polysaccharides, protein and polymers have exhibited the unique advantages for the colon-targeting delivery of several phytochemicals, these systems generally only encapsulate one or two agents (Sun M et al., 2022; Liu et al., 2023). Additionally, the high ratio of excipients and the immature industrialization of these NPs (Nanoparticles) or MPs (Microparticle) greatly restrict their application (Shi et al., 2020; Zoya et al., 2021). The co-delivery of multiple components to specific tissue has become a bottleneck in drug delivery (Gao et al., 2022; Wu Y et al., 2022). Nanoemulsion (droplet diameter of 20 to 200 nm) is an alternative drug delivery system to achieve safe formulations for these poorly soluble compounds and to improve their biopharmaceutical properties and pharmacokinetics (A et al., 2021). As transparent/translucent and dynamically stable dispersion system formed by water, oil and surfactant (Singh et al., 2017), nanoemulsion has been utilized extensively in the pharmaceutical industry. Some previous studies have reported the successful application of nanoemulsion system in UC treatment. Mehrez et al. prepared Malva parviflora leaves extract as nanoemulsion and mixed it with yogurt, enhancing its protective effect on acetic acid-induced UC rats (El-Naggar et al., 2020). Dou et al. prepared bruceine

D as a Self-nanoemulsifying drug delivery system, which improved oral bioavailability and anti-UC effect (Dou et al., 2018). Yen et al. developed nanoemulsion delivery system for andrographolide, which not only improved its oral bioavailability, but also significantly improved its protective effect on inflammatory bowel disease (Yen et al., 2018). However, to the best of our knowledge, there is no report on the development of herbal extract nanoemulsion for DSS-induced UC treatment.

As proof of concept, herein we developed an oral nanoemulsion of HLHP extract (HLHPEN) for multiple components co-delivery, with the enhanced solubility, bioavailability and anti-UC efficacy. Firstly, the formulation of HLHPEN was optimized by pseudo-ternary phase diagram combined with Box-Behnken design. Based on a series of characterization including particle size, TEM morphology, entrapment efficiency of multiple components, and the simulative gastrointestinal stability, HLHPEN was administrated to DSS-induced UC mice, to evaluate the anti-UC efficacy compared to free HLHP extract (HLHPE). This study aimed to develop a new nanoemulsion formulation to improve the water solubility, stability, oral absorption, and UC inhibition effects of TCM herbal extract containing multiple phytochemicals.

Material and methods

Materials

Rhizoma Coptidis (HL, LOT 2007059) was purchased from Sichuan Xinhehua traditional Chinese medicine decoction pieces Co. Ltd (Chengdu, China). *Cortex Magnoliae Officinalis* (HP, LOT 2021120301) was purchased from Anguo YaoYuan Trading Co., Ltd (Baoding, China). Castor oil, soybean oil, olive oil, oleic acid, ethyl oleate, palmitic acid isopropyl ester, tween 80, span 80, ethanol, polyethylene glycol-400, glycerol, 1,3 butanediol and 1.2-propylene glycol were purchased from Chengdu Cologne Chemicals Co., Ltd (Chengdu, China). Polyoxyethylene castor oil (EL-40), polyoxyethylene castor oil (EL-30), octaphenyl polyoxyethyiene (OP-10), caprylic capric triglyceride, propylene glycol caprylate (capryol 90) and Isopropyl myristate were purchased from Shandong Usolf Chemical Technology Co., Ltd (Shangdong, China). Labrasol, LABRAFIL M1944 CS, maisine CC were presented by GATTEFOSSé (Shanghai) Trading Co., Ltd (Shanghai, China). Dextran sulfate Sodium (DSS MW 500 kDa) was purchased from Seebio Biotechnology Co., Ltd (Shanghai, China). Berberine, epiberberine, coptisine, bamatine, magnolol and honokiol were purchased from Chengdu Alfa Biotechnology Co., Ltd (Chengdu, China).

Preparation of HLHP extract

The extraction method was optimized by orthogonal experiments as shown in the supplementary document. HL (40 g) and HP (40 g) were refluxed and extracted twice, with 800 mL of 50% ethanol for 60 min at a time. After decompression and concentration at 60 °C, the dried powder obtained by freeze-drying was HLHPE.

Chemical components analysis by analysis

Due to the differences of physical and chemical properties between components, the main components of HL and HP in the extract were determined by different mobile phases and detection wavelengths. According to the literature review, HLHPE mainly contained alkaloids and lignans, so berberine, epiberberine, coptisine, bamatine, magnolol and honokiol are selected as the indicator components. With acetonitrile-0.05 mol/L potassium dihydrogen phosphate solution (50:50) (0.4 g sodium dodecyl sulfate per 100 mL and phosphoric acid was added to pH 4.0) as the mobile phase, and the detection wavelength was 345 nm to determine the content of alkaloids (berberine, epiberberine, coptisine and bamatine) in HLHPE. Methanol-water (78:22) was used as the mobile phase and the detection wavelength was 294 nm to determine the contents of lignans (magnolol and honokiol) in HLHPE. The flow rate, 1 mL/min. Injection volume, 10 μL. Column temperature, 35 °C.

Preparation of nanoemulsion of HLHP extract (HLHPEN)

In order to further improve the dispersion uniformity of each component in HLHPE, the HLHPEN was prepared by stirring and high-pressure homogenization. In short, distilled water was added dropwise to a mixture of oil, surfactant, cosurfactants and HLHPE under gentle magnetic stirring at 37 °C, then the mixture was homogenized under high pressure at 750 rpm for 20 times to obtain the nanoemulsion. It is filtered by 0.45 μm microporous membrane to obtain the final HLHPEN.

Preliminary screening of HLHPEN prescription

With the content of main components in HLHPE as the index, screen the types of oil, surfactant and cosurfactant. See the supplementary documents for the experimental methods and results (Ma et al., 2022).

The proportion range of oil phase, surfactant and cosurfactant to form nanoemulsion was screened with particle size as index. The ratio of surfactant and cosurfactant was considered to be Km value. After the fixed Km value is 4:1, the surfactant and cosurfactant are mixed to form a mixture of surfactant (Smix). The oil phase and Smix were mixed in the proportions of 1:9, 2:8, 3:7, 4:6, and 5:5 respectively to form a preliminary mixture (Pmix). 15 mL of water was injected into the Pmix, and a series of blank nano emulsions were prepared by high-pressure homogenization. Then, when Km values are 3:1, 2:1, 1:1, 1:2 respectively, other blank nano emulsions are prepared in the same way, and their particle sizes and PDI values are determined. The pseudo three-phase diagram of oil phase, surfactant and cosurfactant was drawn with the particle size of nano emulsion < 100 nm as the index (Zheng et al., 2022).

The methods for optimizing the amount of water phase and HLHPE also were showed in the supplementary document.

With the PDI < 20% as indicators, the rotational speed and times of high-pressure homogenization are optimized in combination with the actual production.

Table 1. Variables in design for the preparation of HLHPEN.

Factors	Level used, actual (coded)		
Independent variables	Low (-1)	Medium (0)	High (+1)
X_1 = Oil/Pmix (%)	6.7%	10%	13.3%
X_2 = Km	1:2	1:1	2:1
X_3 = HLHPE (mg)	160	320	640
Dependent variables	Low	High	Target
Y_1 = Size (nm)	65.46	86.98	minimum
Y_2 = PDI (%)	11.4	26.8	minimum
Y_3 = EE (%)	77.93	99.84	maximum

Optimization of HLHPEN prescription by Box-Behnken design

Through preliminary screening, the dosage range of each material has been basically determined. The formulation of HLHPEN was further optimized by Box-Behnken statistical design (Design Expert®, version 10.0.7, State Ease Inc., USA), in order to determine the optimal proportion of HLHPEN (Kumbhar et al., 2020). The optimization of HLHPEN was carried out by 3-factor, 3-level Box-Behnken Design approach. Based on the preliminary screening result, oil/Pmix (X_1), Km (X_2), and dosage of HLHPE (X_3) were selected as the independent variables. Additionally, particle size (Y_1), PDI value (Y_2), and EE (Y_3) were set as dependent variables (EE refers to the encapsulation efficiency of the total content of berberine, epiberberine, coptisine, bamatine, magnolol and honokiol in HLHPE). Seventeen formulations were prepared by the Box-Behnken design (Table 1).

After the best preparation process of HLHPEN was determined, three batches of HLHPEN were prepared with the best process parameters, and their particle size, PDI value and EE were determined.

Characterization of HLHPEN

After preparing the dilution sample with deionized water for 1:100 ratio, the particle size distribution and PDI of HLHPEN were measured using a dynamic light scattering (DLS) instrument (LITESIZER 500, Anton Paar, Austria). The morphology of particles in HLHPEN was observed by transmission electron microscope (TEM, JEM-1400plus, Tokyo, Japan). 0.1 ml of HLHPEN sample was dropped on the copper mesh, stained with 2% phosphotungstic acid aqueous solution for 10 min. After air drying, the TEM images were collected (Moolakkadath et al., 2020).

5 mL of HLHPEN was taken out and placed in a centrifuge tube containing 3 KDa ultrafiltration membrane, centrifuged at 12000 rpm for 20 min (25 °C), to collect the lower layer of ultrafiltration fluid containing uncoated active components, which was an uncoated HLHPE sample (Hsu & Chen, 2022). The 1 mL HLHPEN, uncoated HLHPE was fixed to 4 mL with methanol respectively, fully demulsified with ultrasound for 10 min, filtered with 0.22 μm microporous filter membrane, and determined according to the HPLC method above-mentioned. The encapsulation efficiency of total content of berberine, epiberberine, coptisine, bamatine, magnolol and honokiol in HLHPE (EE, %) was calculated using Eq. (1). Loading efficiency (LE) of HLHPE was calculated using Eq.(2)

EE (%) = (Total active components in HLHPEN - Active components in uncoated HLHPE)/Total active components in HLHPEN × 100% (1)

LE (%) = Content of HLHPE in HLHPEN/(Content of HLHPE in HLHPEN + Content of carrier in HLHPEN) × 100% (2)

Stability study of HLHPEN

The stability of nanoemulsion would be one of the most important properties. Herein, the centrifugation test, temperature factor, preliminary stability for 3-month storage, as well as the stability in the mimetic gastrointestinal buffer were implemented to evaluate the stability of HLHPEN.

Centrifugation stability

Three batches of HLHPEN were prepared, and then centrifuged at 5000 rpm for 30 min. Whether the unstable signs such as phase separation, emulsification and/or cracking were observed. Meanwhile, the particle size and PDI of HLHPEN before and after centrifugation were measured.

Cold-hot alternate stability

Three batches of HLHPEN were prepared, and placed in a refrigerator at 4 ± 2 °C for 24 h, then taken out and placed in an environment at 25 °C for 24 h, and finally transferred to a water bath at 60 °C for 24 h. Whether the unstable signs such as phase separation, emulsification and/or cracking were observed. Meanwhile, the particle size and PDI of HLHPEN at each temperature were measured.

Preliminary storage stability

Three batches of HLHPEN were prepared, and stored at 25 ± 2 °C and 60 ± 10% relative humidity. Whether the unstable signs such as phase separation, emulsification and/or cracking were observed. Meanwhile, the particle size and PDI of HLHPEN were measured at 1,2,3,4,5,6,7,30,60,90 days, respectively (Galvão et al., 2018).

Gastrointestinal stability in vitro

In order to observe the stability of HLHPEN in the gastrointestinal tract directly, 10 mL HLHPEN was put into a dialysis bag (5000 molecular weight), placed in a simulated solution of the gastrointestinal tract from gastric to small intestine to colon (0~2 h in SGF, 2~6 h in SIF, 6~48 h in SCF), and kept in a shaking water bath at 37 °C and 100 rpm. At a predetermined time (0.5, 1, 1.5, 2, 4, 6, 8, 10, 12, 14, 24, 36 and 48 h), the 0.5 mL HLHPEN in the dialysis bag was taken out. The particle size and PDI of HLHPEN were measured.

Drug release profiles in vitro

The release profile of berberine, epiberberine, coptisine, bamatine, magnolol and honokiol from free HLHPE, and HLHPEN was determined in a simulated fluid environment from gastric to small intestine to colon (0~2 h in SGF, 2~6 h in SIF, 6~48 h in SCF). Then, 0.5% w/v Tween-80 was added to the simulated solution to facilitate the dissolution of berberine, epiberberine, coptisine, bamatine, magnolol and honokiol. The sample was put into a dialysis bag to put into a container containing 40 mL of simulated solution, and placed in a shaker at 37 °C and 100 rpm. At a predetermined time, 1 mL of the simulated solution was taken out and the same volume of a new simulated solution was supplemented. About 1 mL of liquid was extracted with 3 mL of methanol by ultrasonic extraction for 10 min. After filtration, the content of berberine, epiberberine, coptisine, bamatine, magnolol and honokiol was determined by HPLC as mentioned above. This procedure was repeated 3 times for each sample (Li Q et al., 2015; Jain et al., 2023).

Anti-UC effect of HLHPEN in DSS-induced mice

Experimental animals

Male ICR mice with a body weight of 22-25 g were obtained from SPF (Beijing) Biotechnology Co., Ltd (production license number: SCXK-2019-0002). All in vivo experiments were carried out under the guidelines approved by the State Committee of Science and Technology of China and the Institutional Animal Care and Use Committee (IACUC) of Sichuan Province, with permission certificate registration number (SYXK (Chuan) 2020-124).

Efficacy studies of HLHPEN

ICR male mice were randomly divided into 5 groups (n = 12): Control, UC model, 5-ASA, free HLHPE and HLHPEN. The mice in control without any treatment, but mice in other groups were free to drink 3% (W/V) DSS solution for 7 days. After 3 days, mice in the control group and the UC model group were daily orally administrated normal saline, and mice with colitis in other groups were daily orally administrated with 5-ASA (25 mg/kg), free HLHPE (40 mg/kg), HLHPEN (HLHP 40 mg/kg) for 7 days. According to previous reports, the weight, DAI and survival rate of mice were recorded every day from the first day of modeling. after the administration for 7 days, the mice were euthanized with excessive sodium pentobarbital, and the colon tissues were collected and its length was measured (Wang X et al., 2021).

The colon tissue of mice was fixed in 4% paraformaldehyde, embedded in paraffin, and sectioned for 5 μm, and were stained with H&E and PAS respectively. To observe the infiltration degree of inflammatory cells and the distribution of mucus embedded cells in different groups of colon tissues under the microscope (a Leica DM 4000, Germany).

The protein content in colon tissue was determined with the BCA kits from Beyotime Biotech, Co., Ltd (Shanghai China). The IL-6, TNF-α, IL-1β, and IL-10 in colon tissue were tested using ELISA kits from MULLT SCIENCES (LIANKE) Biotech, Co., Ltd. (Huangzhou, China)

Statistical analysis

Statistical analysis of the data between different groups was performed using Graphpad prism 8.0.1 (Graphpad software 8, La Jolla California USA). One-way analysis of variance (ANOVA) was used for multiple groups. A *p < 0.05 indicated that there is a significant difference between the two groups. All

Results

HPLC chromatogram of active components in HLHPE

HLHPE mainly contained alkaloids, lignans, simple phenylpropyl compounds, essential oils and other components, among which the contents of alkaloids and lignans were relatively large (Wang J et al., 2019). Therefore, berberine, epiberberine, coptisine, bamatine in alkaloids, magnolol and honokiol in lignans were selected as indicators for the content determination of HLHPE. The chromatogram is shown in Figure 1, the separation of each index component was good, and the retention time of each peak was also matched with 6 standards. After the extraction with the optimal process, the content of active components was tested and parallel tests were conducted for 3 times. The total content of active components in HLHPE was 31.06 ± 0.96%, including 2.88 ± 0.01% of epiberberine, 5.10 ± 0.01% of coptisine, 4.49 ± 0.01% of bamatine, 16.83 ± 0.04% of berberine, 0.67 ± 0.01% of honokiol and 1.09 ± 0.01% of magnolol.

The alkaloids contained in HLHPE have strong polarity, so the retention time on the reversed-phase chromatographic column was too short. In addition, epiberberine, coptisine, balmatine, and berberine were difficult to separate due to their similar structures, so ion pair containing reagents were selected as mobile phases to determine the content of alkaloids (Xie L et al., 2021). The polarity of lignans in HLHPE is small, and it could be well separated by methanol-water mobile phase (Wu Q et al., 2019). Therefore, two mobile phases were used to determine the content of main components in HLHPE.

Optimization of HLHPEN prescription

Nanoemulsion can be prepared by two methods: low-energy emulsion and high-energy emulsion (Singh et al., 2017; Ghazy et al., 2021). Among them, low-energy emulsion will be greatly limited by the type of oil and emulsifier, while high-energy emulsion is almost suitable for the preparation of all oil phases

(Singh et al., 2017). High pressure homogenization and ultrasonic are the main ways of high-energy emulsification. Because the components of HLHPE were complex, and high-pressure homogenization could achieve nondifferential shearing of multiple components, high-pressure homogenization is suitable for the preparation of HLHPEN in this study.

The screening results of oil, surfactant and cosurfactant types are shown in Figure S1. It is determined that oleic acid is the oil phase, EL40 is the surfactant and PEG400 is the cosurfactant. They not only had relatively high solubility to HLHPE, but also had good safety (Hsu & Chen, 2022). The results of the addition amount of water and HLHPE were shown in Figure S2. It was clear shown that the proportion of distilled water in nanomulsion is 67%, the addition amount of HLHPE was further optimized in 160, 320, 640 mg. Through pseudo-ternary phase diagram, we determined an appropriate range of each dosage of oil, surfactant and cosurfactant for forming blank nanoemulsion. Figure 2A–E showed the appearance, particle size and PDI of blank nanomulsion with Km values of 4:1, 3:1, 2:1, 1:1 and 1:2 respectively. Oleic acid, EL40 and PEG400 have good ability to form nanoemulsion under the appropriate ratio. It could be seen from Figure 2F that when the amount of the oil phase is 1 0~50% w/w, the amount of the surfactant is 5 0~90% w/w, and the amount of the cosurfactant is 2 0~60% w/w, the particle size formed is less than 100 nm, and the PDI is less than 30%, indicating that the blank nanomulsion with uniform particle size is formed.

At a suitable rotational speed, through repeated high-pressure homogenization, the nanomulsion gradually forms a uniform and suitable particle size (Harun et al., 2018). As shown in Figure 2G, H, the optimal number of cycles for high-pressure homogenization of HLHPEN is 15, and the optimal flow rate is 750 rpm.

The optimal proportion of HLHPEN was obtained by Box-Behnken statistical design. The particle size, PDI and EE of HLHPEN directly affect the stability and effectiveness of the formulation (Qushawy et al., 2022). It is necessary to clarify the corresponding relationship between the proportion of each phase in HLHPEN and the particle size, PDI and EE (Subongkot & Ngawhirunpat, 2017).Therefore, Box-Behnken designed 17
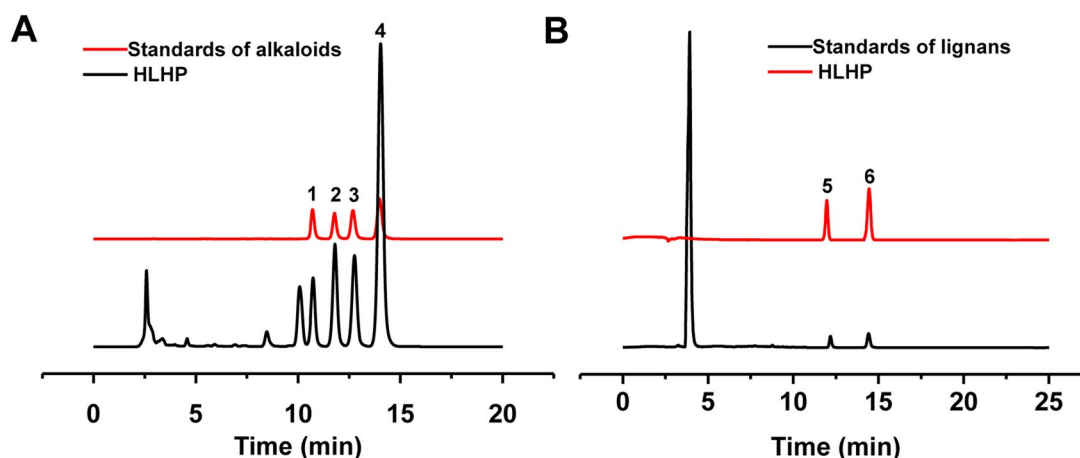

Figure 1. HPLC chromatogram spectra of HLHPE, based on the different analysis conditions of alkaloids (A) and lignans (B). Peak 1~6 represents as epiberberine, coptisine, balmatine, berberine, honokiol, magnolol, respectively.
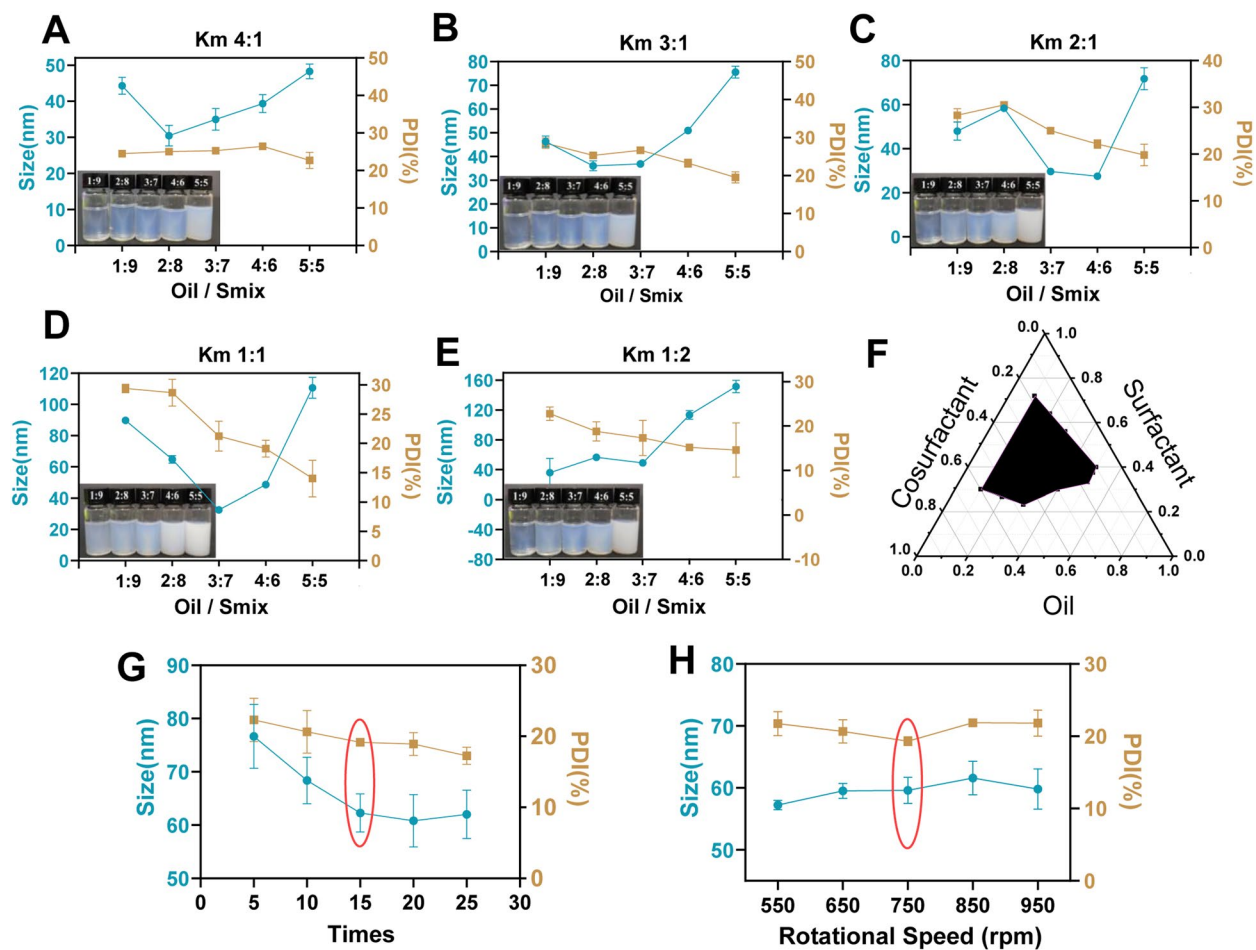
Figure 2. Particle size, PDI and pseudo-ternary phase diagram of oleic acid/EL40/PEG400 prepared blank nanomulsion. (A) Km 4:1. (B) Km 3:1. (C) Km 2:1. (D) Km 1:1. (E) Km 1:2. (F) Pseudo-ternary phase diagram with particle size less than 100 nm ($n = 3$). (G) Times of high-pressure homogenization. (H) Rotational speed of high-pressure homogenization.

Table 2. The level of independent variables, dependent variables and regression analysis results of experimental operation in Box-Behnken design.

Batch	Values of independent variables			Dependent variables responses		
	X_1(% w/w)	X_2	X_3(mg)	Y1(nm)	Y2(%)	Y3(% w/w)
1	1	1	0	82.7	15.4	90.36
2	−1	0	−1	58.41	26.7	94.51
3	1	0	1	64.36	15.5	90.85
4	−1	−1	0	69.51	24.4	84.87
5	0	1	1	71.97	20.1	91.86
6	1	−1	0	57.74	11.4	82.77
7	0	0	0	78.19	19.4	82.33
8	0	−1	−1	70.46	26.8	98.53
9	0	1	−1	68.82	20.1	94.49
10	0	−1	1	62.16	19.6	87.43
11	−1	0	1	54.28	21.5	84.1
12	0	0	0	77.62	18.8	82.7
13	0	0	0	78.86	18.9	82.46
14	0	0	0	78.48	18.4	83.58
15	−1	1	0	53.35	15.3	77.93
16	1	0	−1	71.02	20.8	99.84
17	0	0	0	76.67	18.2	83.31
Quadratic model	R^2	Adjusted R^2	Predicted R^2	SD	%CV	
Response(Y_1)	0.9909	0.9792	0.9512	1.17	1.64	
Response(Y_2)	0.9902	0.9775	0.8921	0.60	3.63	
Response(Y_3)	0.9914	0.9803	0.8886	0.89	1.02	

batches of tests to study the influence of independent variable (oil/Pmix, Km, HLHPE) on dependent variable (Size, PDI, EE). The details of each batch of tests are shown in Table 2.

Effect of independent factors on size, PDI and EE

The particle size of 17 batches of HLHPEN ranged from 63.35 ± 1.47 nm to 88.86 ± 2.71 nm, the PDI from 11.4% ± 2.8%

to 26.8% ± 5.1%, and EE ranged from 77.93% to 99.84%. It was found that the best fit model of HLHPEN was a quadratic model. The model is significant ($p < 0.0001$), but the F-value of Lack of Fit is not significant, and the difference between the predicted and adjusted R^2 of particle size is less than 0.2, indicating that the model can be used to predict the design space.

$$Y_1(\text{Size}) = +87.96 + 7.78 * X_1 - 2.75 * X_2 + 0.38 * X_3 + 4.78 * X_1 X_2$$
$$+ 1.37 * X_1 X_3 + 1.11 * X_2 X_3 - 8.11 * X_1^2 - 0.53 X_2^2 - 4.83 * X_3^2 \quad (3)$$

$$Y_2(\text{PDI}) = +15.74 - 3.10 * X_1 - 1.41 * X_2 - 2.21 * X_3 + 3.27 * X_1 X_2$$
$$- 0.025 * X_1 X_3 + 1.80 * X_2 X_3 - 1.32 * X_1^2 - 0.80 * X_2^2 + 3.71 * X_3^2 \quad (4)$$

$$Y_3(\text{EE}) = +82.87 + 2.80 * X_1 + 0.13 * X_2 - 4.14 * X_3$$
$$+ 3.63 * X_1 X_2 + 0.36 * X_1 X_3 + 2.12 * X_2 X_3$$
$$+ 0.18 * X_1^2 + 0.93 * X_2^2 + 9.27 * X_3^2 \quad (5)$$

In the polynomial equation (3), X_1 had a significant effect on particle size ($p < 0.001$). It could be seen from Figure 3A that the particle size of HLHPEN gradually increased with the increase of oil/Pmix. In addition, the influence of X_2 on the particle size was also significant ($p < 0.05$). With the increase of Km, the particle size of HLHPEN decreased. This was consistent with the previous conclusion that the particle size of nanoemulsion decreased with the increased of surfactant. After the parent droplet is broken, the newly formed droplets can remain stable as long as there are enough surfactants covering a large interface and the time scale of surfactant adsorption is smaller than the aggregation scale (Ravanfar et al., 2016).

In the polynomial equation (4), X_1 and X_3 had a significant effect on PDI ($p < 0.001$). It can be seen from Figure 3B that the PDI of HLHPEN gradually decreases with the increase of oil/Pmix, While PDI decreased first and then increased with the increase of HLHPE dosage. With the increase of Km, the PDI of HLHPEN also decreased. This is also related to the surfactant stabilizing the droplet interface (Blasi et al., 2011).

In the polynomial equation (5), X_1 and X_3 had a significant effect on EE ($p < 0.001$). It can be seen from Figure 3C that the EE of HLHPEN gradually decreases with the increase of HLHPE dosage, while the EE of HLHPEN gradually increases with the increase of oil/Pmix. This would be that the increase of oil phase can increase the solubility of liposoluble components in HLHPE, making it easier to wrap in Oil droplets, thus improving the EE of HLHPEN.

Based on the Box-Behnken design, it was found that the software predicted values of particle size (Figure 3D), PDI (Figure 3E) and EE (Figure 3F) were basically distributed in a straight line with the actual measured values, indicating that the model had good predictability. Figure 3G showed the appearance of 17 batches of samples, and the optimal formulation of HLHPEN was obtained based on the criteria of minimum particle size, minimum PDI and maximum EE. The independent variables of the optimized formula are oil/Pmix −0.825, Km 1, HLHPE −1. The formula of HLHPEN should be: oleic acid 7.28%, EL-40 17.34%, PEG400 8.67%, water 66.7%, HLHPE 160 mg in 45 g HLHPEN. The predicted particle size of the microemulsion was 63.35 nm, the PDI was 19.56%, and the EE was 90.28%.

Characterization of HLHPEN

HLHPEN was prepared according to the optimized formulation of Box-Behnken design. The appearance of HLHPEN as shown in Figure 4A was brownish yellow, clear and transparent liquid. As an O/W nanoemulsion, HLHPEN obtained by infinitely diluting with water. As shown in Figure 4B, the particle size was 65.21 ± 0.82 nm and PDI was 18.28 ± 1.69%, the EE was 90.64 ± 0.19% and LE was 1.05% of HLHPEN, which was close to the size, PDI and EE predicted by Design Expert® software. According to the different polarity of the compounds contained in HLHPE, its encapsulation efficiency in nanoparticles was also different. The EE of epiberberine was 91.50%, LE 0.03%; the EE of coptisine was 91.48%, LE 0.05%; the EE of bamatine was 91.96%, LE 0.05%; the EE of berberine was 88.70%, LE 0.16%, and the EE of honokiol was 99.95%, LE 0.01%; the EE of magnolol is 99.96%, its LE 0.02%. The results showed that the smaller the polarity of the component, the higher its encapsulation efficiency. Berberine had the lowest entrapment rate, which was related to its highest content in HLHPE. The total LE of the index component is 0.32%, and the content of the index components has been determined to be 31.06% of HLHPE by HPLC analysis, so the drug loading rate of the extract is 1.05%.

In addition, the TEM microscopic morphology is shown in Figure 4C, which is in the shape of a nearly circular droplet, and the distribution is relatively uniform. As shown in Figure 4A, with the help of mixed surfactants, oleic acid accumulates into droplets, with the hydrophobic end inside and the hydrophilic part outside, to form nanoemulsion. The liposolubility components represented by honokiol and honokiol were completely dissolved in the oleic acid at the hydrophobic end, while the components with higher polarity represented by berberine were partially dissolved and wrapped in oleic acid with the help of emulsifiers. Therefore, nano-emulsions could effectively load components with different solubility at the same time.

When the particle size changes little, the interfacial equilibrium of the surface nanomulsion is not destroyed. In addition, when the PDI value remains below 20%, it indicates that the system is uniform and stable (Galvão et al., 2018). The centrifugal stability study found (Figure 4D) that after centrifugation, HLHPEN was not layered, and still a brownish yellow uniform liquid with no significant change in particle size and PDI, indicating that the modified formulation had good centrifugal stability. In the cold-hot alternation stability study (Figure 4E), HLHPEN was stable at 4 °C and 25 °C, with little change in particle size and PDI. However, after treatment at 60 °C, the particle size of HLHPEN increased significantly, from 67.61 nm to 1141.4 nm, indicating that HLHPEN was not stable at 60 °C, and high temperature would damage its structure. The preliminary storage stability study found (Figure 4F) that the particle size and PDI of HLHPEN did not change much within 90 days under normal temperature conditions, indicating it has good storage stability.

Gastrointestinal stability and drug release profiles in vitro

The pH value and ionic strength of gastrointestinal environment affect the solubility of components, change the
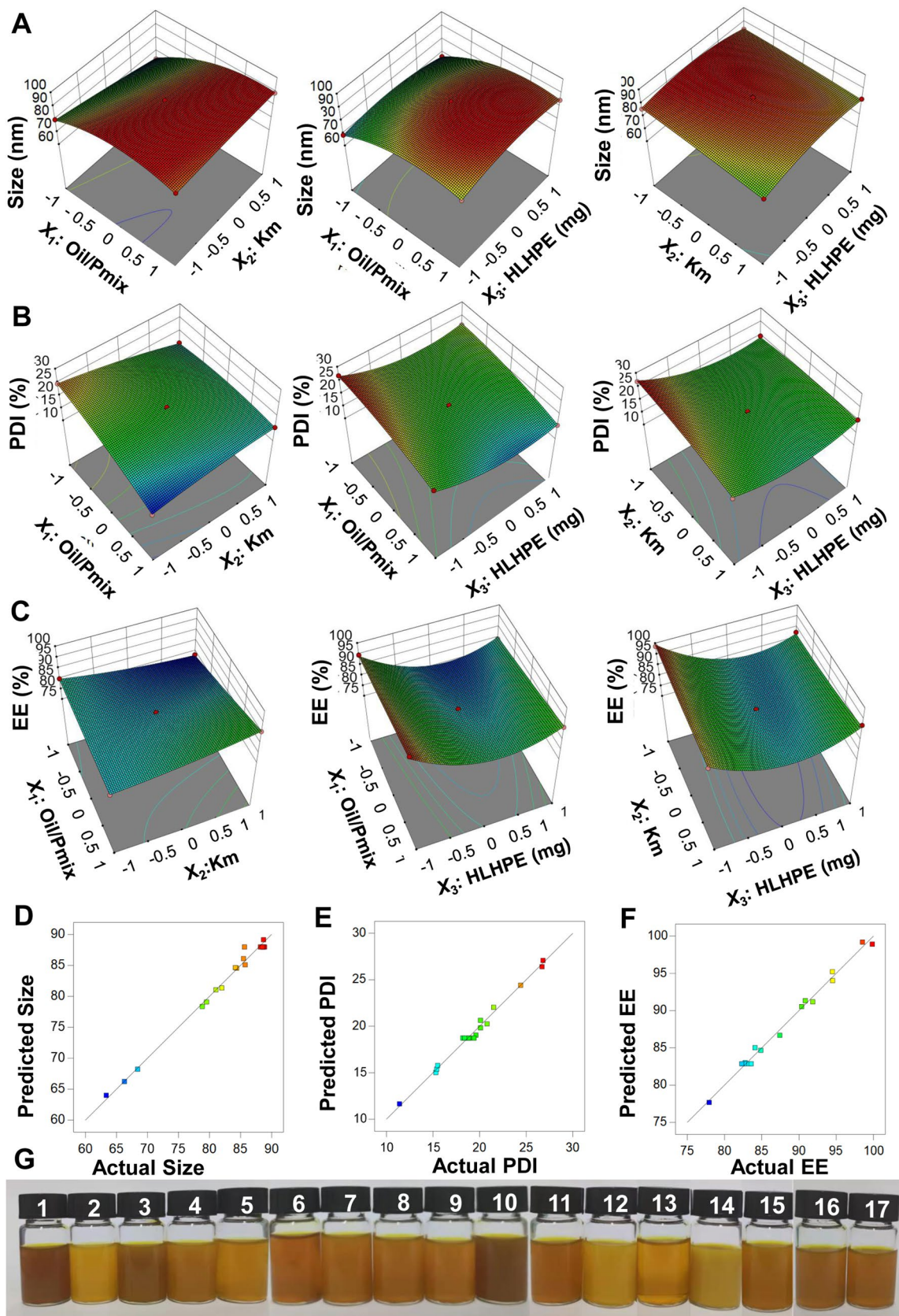
Figure 3. Three-dimensional surface response plots showing effect of oil/Pmix, Km and HLHPE on (A) Particle size, (B) PDI, (C) EE. Linear correlation plots between the actual and predicted values for (D) particle size. (E) PDI. (F) EE. (G) appearance of 17 batches of HLHPEN.

distribution of oil-water interface, which resultantly affected the stability of nanoemulsion (Zhu et al., 2021). Many components in HLHPE are unstable in the gastrointestinal tract and easy to be degraded and lose efficacy, such as berberine. It reported that 99.5% of berberine in oral doses disappeared during the gastrointestinal first-pass elimination process
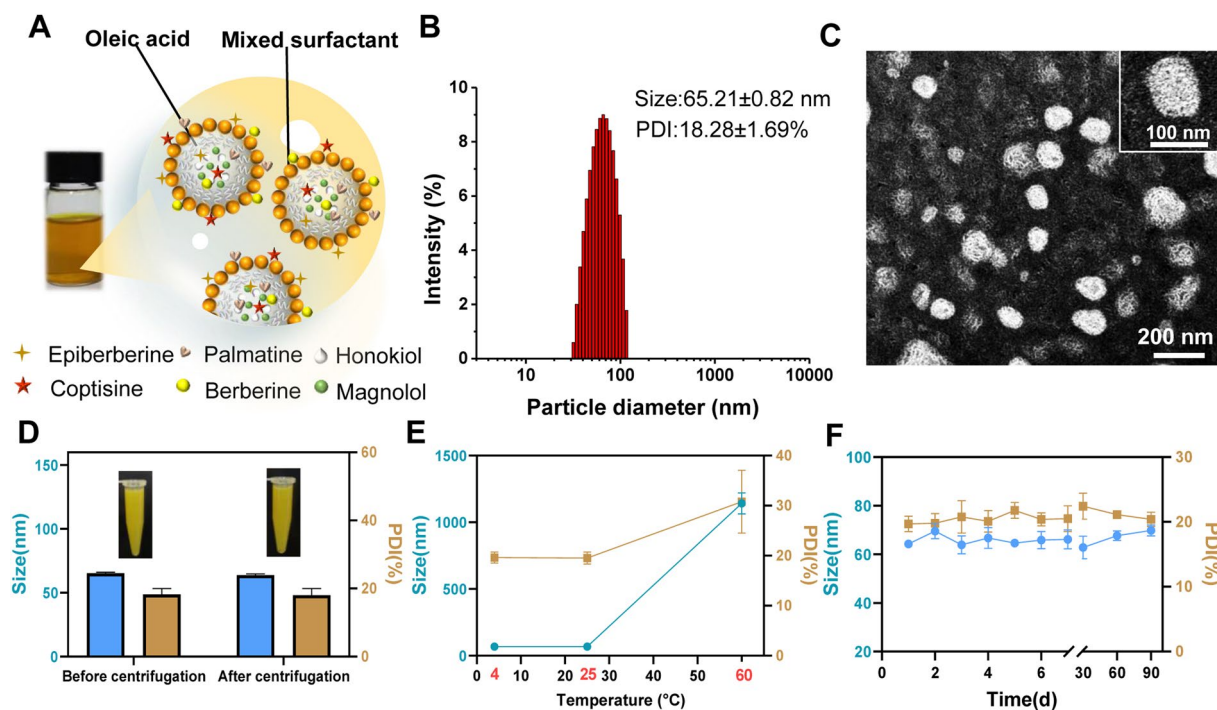
Figure 4. Characterization of HLHPEN. (A) Schematic diagram of HLHPEN structure. (B) Particle diameter and PDI of HLHPEN. (C) TEM diagram of HLHPEN. (D) Centrifugation stability of HLHPEN. (E) Cold-hot alternate stability of HLHPEN. (F) Storage stability of HLHPEN.
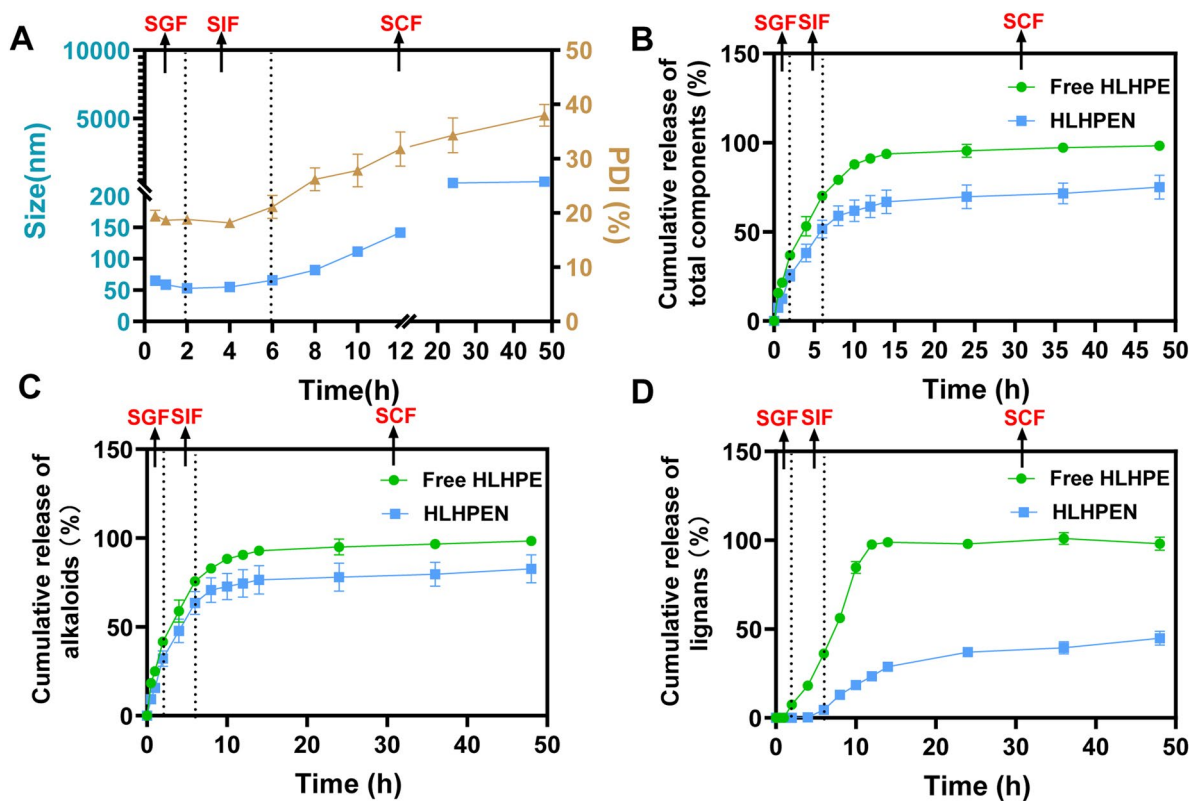

Figure 5. Gastrointestinal stability and drug release profiles of HLHPE *in vitro*. (A) Size and PDI changes. (B)Cumulative release of total components. (C) Cumulative release of alkaloids. (D) Cumulative release of lignans.

(Kwon et al., 2020). As showed in Figure 5A, the particle size and PDI value of the HLHPEN changed little within 2 h in SGF, gradually increased in SIF, and sharply increased in SCF, indicating that HLHPEN could exist stably in gastric juice and

intestinal juice, and its nanostructure was not completely destroyed until it was in SCF.

The drug delivery profiles of HLHPE and HLHPEN was also studied under simulated gastrointestinal conditions, as

depicted in Figure 5. The burst release was found for total components with 36.87%, alkaloids with 41.67%, lignans with 7.45% of free HLHPE release within 2 h in SGF owing to the initial large concentration gradient across the dialysis membrane, followed by a rapid release over the next 4 h in SIF and achieving the cumulative percentage of total components with 70.14%, alkaloids with 75.69%, and lignans with 36.20% of free HLHPE. Finally, at 12 h in SCF, the cumulative release rate of total components, alkaloids, lignin was 91.06%, 90.54%, 97.56%, respectively. In contrast, HLHPE prepared as nanoemulsion significantly delayed its release rate, especially lignans. Only 4.55% of lignans in HLHPEN were released in the 6-h SIF incubation, followed by the cumulative percentages of lignans with 23.34% in the 12-h SCF incubation. In addition, the cumulative release of alkaloids was only 74.43% in 12 h SCF. These results were consistent with the advantages of nanoemulsion, which not only improved the water solubility of HLHPE, but also protected its active components (alkaloids or lignans) from gastrointestinal degradation to delay their release.

Anti-ulcerative colitis effect of HLHPEN in vivo

Colon length, body weight, DAI and survival

Although previous studies have found that HL and HP could improve UC (Xie Q et al., 2022), it is unclear whether their anti-UC effect is enhanced after being prepared as nanoemulsions. The success of DSS induced-UC and the efficacy of the therapeutic groups were evaluated from the disease related indicators of colon length, weight, DAI score and survival rate (Yang et al., 2022). The feeding, modeling and administration methods of mice were shown in Figure 6A. Compared with the control group, the colon length of the DSS induced -UC group in Figure 6B was shortened ($p < 0.05$). After be treated with 5-ASA, free HLHPE and HLHPEN, the colon shortening of mice caused by DSS could be effectively suppressed, and the effect of HLHPEN was the most significant ($p < 0.05$). As shown in Figure 6C, compared with the control group, after drinking DSS, the body weight of mice in each group began to decrease from 4 days, which to a certain extent indicated that the induction of UC model by DSS was successful (Zhang C, Wang X, et al., 2022). After treatment, the weight loss caused by DSS was slowed down. By the 10th day, the weight of mice of the 5-ASA and HLHPEN group was significantly increased compared with that of the UC model group ($p < 0.05$). DAI in Figure 6D included the comprehensive scores of body weight, diarrhea and hematochezia. The higher the severity of ulcerative colitis, the higher the DAI (Zhang C, Li J, et al., 2022). From the third day, except for the control group, the DAI of mice in each group drinking DSS gradually increased, and on the tenth day, the average DAI of UC model group was the highest, and the DAI score of each treatment group was decreased, and the DAI of mice in HLHPEN group was significantly decreased.

As shown in Figure 6E, the survival rate of HLHPEN is 75%, while that of UC model group is only 50%. Therefore, the survival rate could reflect the effect of the treatment drug against DSS induced UC to a certain extent (Zhong et al., 2022). On the other hand, it can also examine the safety of HLHPEN by oral administration. Therefore, from the daily observation indicators, HLHPE had the anti-UC effect, and the preparation of HLHPEN significantly improved its anti-UC effect.
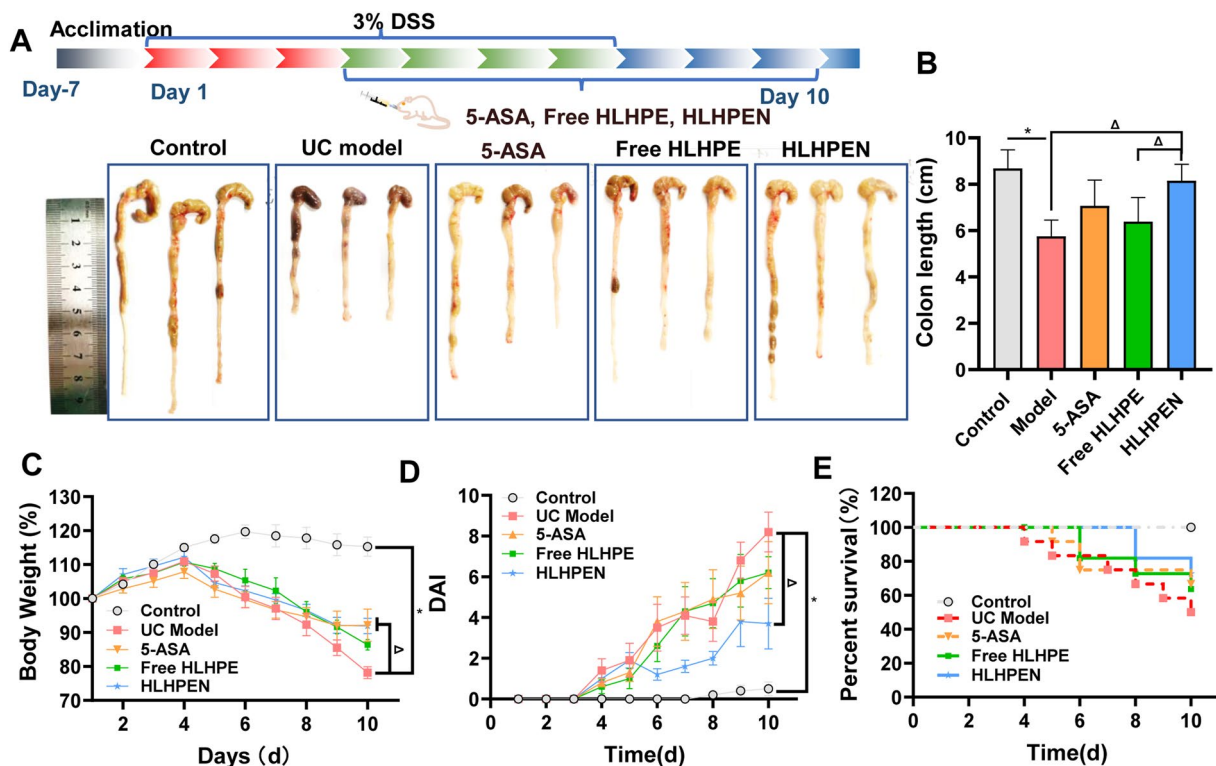

Figure 6. Observed efficacy indexes of HLHPEN on anti-UC effect. (A) Modeling and treatment experiment design and photos of colon. (B)Colon length. (C) Body weight. (D) DAI. (E) Survival Rate. (*$p < 0.05$ vs UC Model, Δ $p < 0.05$ vs HLHPEN).
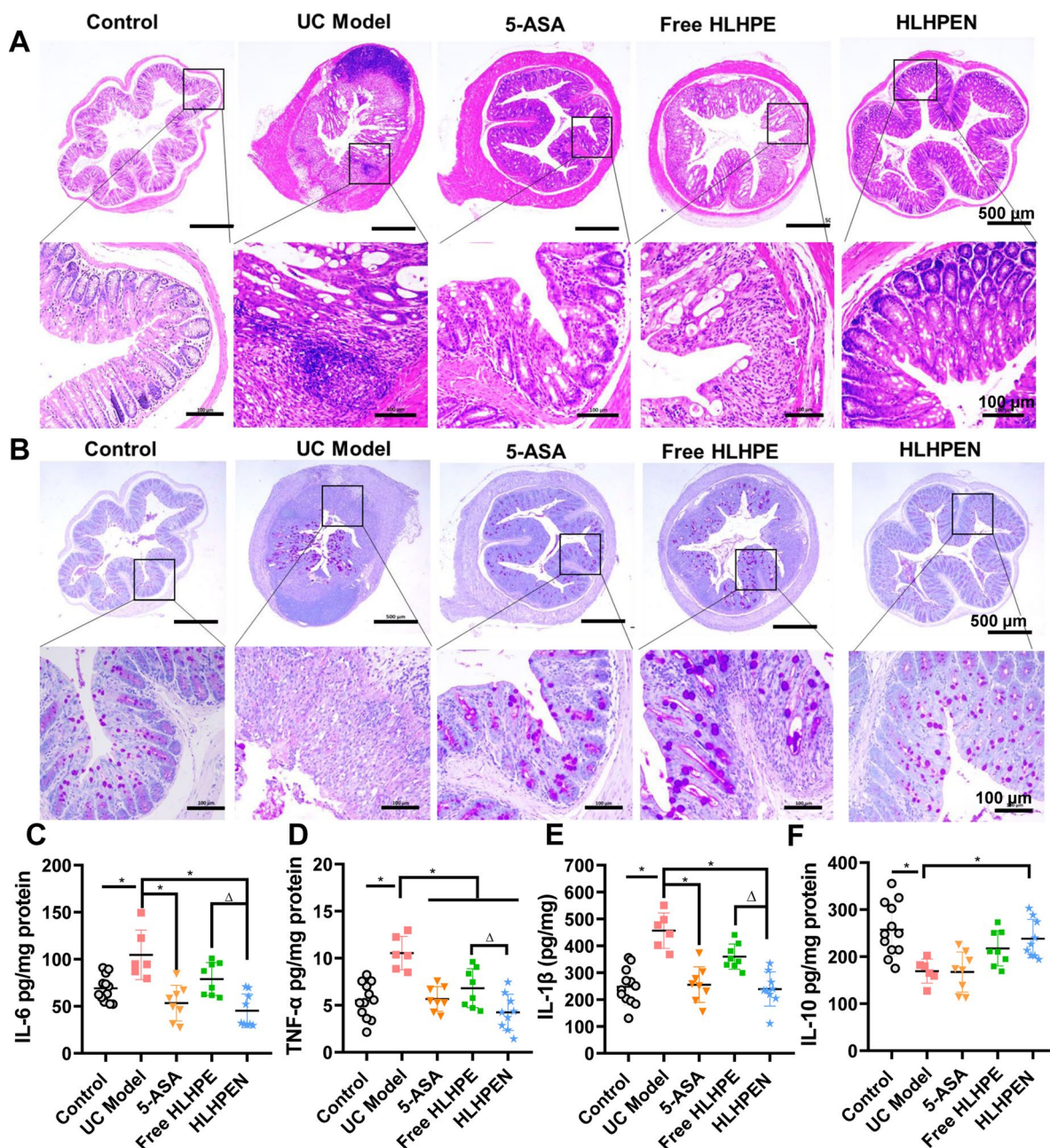
Figure 7. H&E and PAS staining and expression of inflammatory cytokines in colon tissue. (A) H&E staining. (B) PAS staining. (C) Inflammatory cytokines (*p < 0.05 vs UC Model, Δp < 0.05 vs HLHPEN).

H&E and PAS staining

Pathological sections of colon tissue could reveal the severity of UC from the histological level, and H&E staining can observe the infiltration of inflammatory cells in the colon (Liu C et al., 2022). As shown in Figure 7A, compared with the control group, the crypt structure of the colonic mucosa in the UC model group was completely destroyed, the centriole cells in the mucosa and submucosa were aggregated, and obvious edema appeared in the lamina propria. The 5-ASA group protected the integrity of the mucosal structure, but the edema of its lamina propria could not be ignored. The free HLHPE group also alleviated the inflammatory aggregation of DSS on the mucosal layer, but some inflammatory

cells still infiltrated. In HLHPEN group, the structure of colonic mucosa was the most complete, and the boundary between colonic mucosa and submucosa was obvious. There was no edema in lamina propria. It showed that all the treatment groups could alleviate the inflammatory infiltration caused by DSS, and HLHPEN had the best effect.

PAS staining marked glycoproteins in colon tissue thus reflecting the structural integrity of mucus goblet cells in mucosal tissue (Zhang CL et al., 2017). As showed in Figure 7B, compared with the control group, the mucus goblet cells in the colon tissue of the UC model group were completely destroyed, while relatively complete mucus cells remained in other treatment groups, indicating that 5-ASA, free HLHPE

and HLHPEN could maintain the integrity of the colon mucosa. Similarly, HLHPEN had the strongest effect on maintaining mucus goblet cells in colon.

Inflammatory cytokines

UC, as an inflammatory disease, the amounts of inflammatory factors secreted by the colon is closely related to the severity of UC (Ding et al., 2020). Among them, the content of pro-inflammatory factors such as IL-6, TNF-a and IL-1β is positively correlated with the degree of inflammation, while the level of anti-inflammatory factors represented by IL-10 is negatively correlated with the degree of inflammation (Geremia et al., 2014; Zhang C et al., 2021). As shown in Figure 7C–E, compared with the control group, IL-6, TNF-a and IL-1β in UC model group significantly increased, while 5-ASA, free HLHPE and HLHPEN had the effect to inhibit their increasing trend, and the inhibition effect of HLHPEN was most significant ($p < 0.05$). As for the anti-inflammatory factor IL-10 (Figure 7F), the content in UC model group was the lowest, and 5-SAS did not increase the content of IL-10, while both free HLHPE and HLHPEN could increase the content of IL-10, of which HLHPEN increased the most significantly ($p < 0.05$). Therefore, from the perspective of daily disease indicators, pathological sections and inflammatory cytokines, it is confirmed that the preparation of HLHPEN is conducive to improving its anti-inflammatory effect.

Discussion

This study deals with the development of HLHPEN to realize the co-delivery of HLHPE multi-components, improve the solubility of HLHPE, enhance stability and enhance its anti-UC effect. The solubility test preliminarily found that oleic acid in the oil phase has the best solubility for HLHPE. Among the surfactants, span 80 had the largest dissolution, but its emulsification rate for oleic acid is low. EL-40 not only had good solubility for HLHPE, but also had good emulsification ability for oleic acid. In addition, the cosurfactant selects PEG400 with greater safety to further increase the emulsification ability of EL-40. Therefore, oleic acid, EL-40 and PEG400 are finally selected as the main carriers of HLHPEN. The pseudo-three phase diagram was further used to preliminarily screen the prescription proportion, and the suitable range for forming the uniform particle size nanoemulsion was screened out. In combination with Box-Behnken design, the optimal prescription ratio of HLHPEN was further optimized, and the particle size, PDI and encapsulation efficiency of nanoemulsion could be predicted by the best parameters, which improved the drug optimization efficiency (Tripathi et al., 2018). Due to the excellent solubility of oleic acid, EL-40 and PEG400 for multi-components, the prepared HLHPEN had the ability of multi-component co-delivery.

Because of the special location of UC, how to protect the drug to overcome the severe gastrointestinal damage during oral administration has become a key problem in the treatment of UC (Jacob et al., 2020). This study was surprised to found that the HLHPEN has good stability of stomach and small intestine. The analysis of the reasons was mainly due to two points. First, thanks to the optimization of the formula of nano HLHPEN, it was found that oleic acid, EL-40 and PEG400 have the ability to self-emulsify at an appropriate proportion. Under the appropriate temperature and gentle stirring in the stomach, they can easily form diluted self-emulsifying nanoemulsion with the water in the gastric juice, thus protecting drugs from damage of digestive enzymes and extreme pH values (Jain et al., 2013; Jain et al., 2023). The HLHPEN in this study has also been homogenized under high pressure, and its structure was more stable and not easy to be damaged. Second, the stable intestinal transit time made the retention time of nanoemulsion in the stomach and small intestine relatively short, and it could be preserved completely. When the nanoemulsion was delivered to the colon, the structure of the nanoemulsion would be further damaged due to the long transport time, large amount of intestinal water reabsorption, and a large number of microorganisms and digestive enzymes (Kali et al., 2022). Therefore, reasonable nanoemulsion formulation and stable intestinal transit time reduced the drug release of HLHPEN in the stomach and small intestine, but release it in large quantities in the colon, thus playing a good anti UC role.

The efficacy test of anti-UC mice showed that HLHPEN had better therapeutic effect. This was mainly due to the preparation advantages of nanoemulsion. 5-ASA and HLHPE existed in free state, which were inevitably damaged by pH value and digestive enzymes, and had first-pass effect after being absorbed by intestinal capillaries, which reduced the effect. However, after HLHPEN was taken orally, the oil phase contained in it is formed into emulsified monoglycerides, diglycerides and fatty acids under the action of enzymes such as pancreatic lipase. The intestinal mixed micelles formed in the presence of bile acid then pass through intestinal cells (cross cell pathway) and deliver the drug to lymphatic vessels instead of blood vessels (Zeng et al., 2021). When colitis occurred, more macrophages accumulated in the inflammatory site (Sun T et al., 2020), and the colon barrier was destroyed, which was more conducive to the nanoemulsion to cross the cell barrier and directly affect the inflammatory cells to play its role. This transport mode protected HLHPE from the influence of liver first-pass metabolism, increased oral bioavailability and enhanced drug efficacy.

Conclusion

In conclusion, we developed a herbal nanoemulsion, HLHPEN, constituted with 160 mg HLHP extract, 7.28% oleic acid, 17.34% EL-40, 8.67% PEG400, and 66.7% water, based on the pseudo-ternary phase diagram and Box-Behnken design optimization. HLHPEN exhibited the optimal storage stability including the centrifugation, cold-heat circulation, and long-term colloidal stability. Furthermore, HLHPEN manifested the desired gastrointestinal stability and sustained drug release in the simulated gastrointestinal environment, therefore which indicated that it would be a feasible oral nano-scaled formulation. The experimental results on DSS-induced UC mice models showed that compared to free extract, HLHPEN significantly

alleviated UC-related symptoms and pathological state. Thus, the herbal nanoemulsion system represented the promising potential for UC prevention and treatment.

Disclosure statement

No potential conflict of interest was reported by the authors.

Ethical approval statement

All institutional and national guidelines for the care and use of laboratory animals were followed. The ethics committee: the State Committee of Science and Technology of China and the Institutional Animal Care and Use Committee (IACUC) of Sichuan Province.

The number or ID of the ethics approval: SYXK (Chuan) 2020-124.

The mice were used to study the anti-UC effect of the preparation. All mice were under the conditions of room temperature ($20 \pm 0.5°$ C,), humidity ($50 \pm 10\%$), light (12 h light/dark cycle) and were free access to diet. At the end of study, the animals were sacrificed following anesthesia with pentobarbital sodium (80 mg/kg).

Funding

References

A N, Kovooru L, Behera AK, Kumar KPP, Srivastava P. (2021). A critical review of synthesis procedures, applications and future potential of nanoemulsions. Adv Colloid Interface Sci 287:1.

Blasi P, Giovagnoli S, Schoubben A, Puglia C, Bonina F, Rossi C, Ricci M. (2011). Lipid nanoparticles for brain targeting I. Formulation optimization. Int J Pharm 419:287–14.

Ding YF, Sun T, Li S, Huang Q, Yue L, Zhu L, Wang R. (2020). Oral colon-targeted konjac glucomannan hydrogel constructed through noncovalent cross-linking by cucurbit[8]uril for ulcerative colitis therapy. ACS Appl Bio Mater 3:10–9.

Dou YX, Zhou JT, Wang TT, Huang YF, Chen VP, Xie YL, Lin ZX, Gao JS, Su ZR, Zeng HF. (2018). Self-nanoemulsifying drug delivery system of bruceine D: a new approach for anti-ulcerative colitis. Int J Nanomedicine 13:5887–907.

El-Naggar ME, Hussein J, El-sayed SM, Youssef AM, El Bana M, Latif YA, Medhat D. (2020). Protective effect of the functional yogurt based on Malva parviflora leaves extract nanoemulsion on acetic acid-induced ulcerative colitis in rats. J Mater Res Technol 9:14500–8.

Galvão KCS, Vicente AA, Sobral PJA. (2018). Development, characterization, and stability of O/W pepper nanoemulsions produced by high-pressure homogenization. Food Bioprocess Technol 11:355–67.

Gao Q, Feng J, Liu W, Wen C, Wu Y, Liao Q, Zou L, Sui X, Xie T, Zhang J, Hu Y. (2022). Opportunities and challenges for co-delivery nanomedicines based on combination of phytochemicals with chemotherapeutic drugs in cancer treatment. Adv Drug Deliv Rev 188:114445.

Geremia A, Biancheri P, Allan P, Corazza GR, Di Sabatino A. (2014). Innate and adaptive immunity in inflammatory bowel disease. Autoimmun Rev 13:3–10.

Ghazy OA, Fouad MT, Saleh HH, Kholif AE, Morsy TA. (2021). Ultrasound-assisted preparation of anise extract nanoemulsion and its bioactivity against different pathogenic bacteria. Food Chem 341:128259.

Harun SN, Nordin SA, Gani SSA, Shamsuddin AF, Basri M, Basri HB. (2018). Development of nanoemulsion for efficient brain parenteral delivery of cefuroxime: designs, characterizations, and pharmacokinetics. Int J Nanomedicine 13:2571–84.

He Y, Chen Z, Nie X, Wang D, Zhang Q, Peng T, Zhang C, Wu D, Zhang J. (2022). Recent advances in polysaccharides from edible and medicinal Polygonati rhizoma: From bench to market. Int J Biol Macromol 195:102–16.

Hsu HY, Chen BH. (2022). A comparative study on inhibition of breast cancer cells and tumors in mice by carotenoid extract and nanoemulsion prepared from sweet potato (Ipomoea batatas L.) peel. Pharmaceutics 14:980.

Jacob EM, Borah A, Pillai SC, Kumar DS. (2020). Inflammatory bowel disease: The emergence of new trends in lifestyle and nanomedicine as the modern tool for pharmacotherapy. Nanomaterials 10:2460.

Jain S, Jain AK, Pohekar M, Thanki K. (2013). Novel self-emulsifying formulation of quercetin for improved in vivo antioxidant potential: implications for drug-induced cardiotoxicity and nephrotoxicity. Free Radic Biol Med 65:117–30.

Jain S, Kumar N, Sharma R, Date T, Bhargavi N, Chaudhari D, Katiyar SS. (2023). Self-nanoemulsifying formulation for oral delivery of sildenafil: effect on physicochemical attributes and in vivo pharmacokinetics. Drug Deliv Transl Res 13:839–51.

Jing W, Dong S, Luo X, Liu J, Wei B, Du W, Yang L, Luo H, Wang Y, Wang S, Lu H. (2021). Berberine improves colitis by triggering AhR activation by microbial tryptophan catabolites. Pharmacol Res 164:105358.

Kali G, Knoll P, Bernkop-Schnurch A. (2022). Emerging technologies to increase gastrointestinal transit times of drug delivery systems. J Control Release 346:289–99.

Kobayashi T, Siegmund B, Le Berre C, Wei SC, Ferrante M, Shen B, Bernstein CN, Danese S, Peyrin-Biroulet L, Hibi T. (2020). Ulcerative colitis. Nat Rev Dis Primers 6:74.

Kumbhar SA, Kokare CR, Shrivastava B, Gorain B, Choudhury H. (2020). Preparation, characterization, and optimization of asenapine maleate mucoadhesive nanoemulsion using Box-Behnken design: In vitro and in vivo studies for brain targeting. Int J Pharm 586:119499.

Kwon M, Lim DY, Lee CH, Jeon JH, Choi MK, Song IS. (2020). Enhanced intestinal absorption and pharmacokinetic modulation of berberine and its metabolites through the inhibition of P-glycoprotein and intestinal metabolism in rats using a berberine mixed micelle formulation. Pharmaceutics 12:882.

Li C, Ai G, Wang Y, Lu Q, Luo C, Tan L, Lin G, Liu Y, Li Y, Zeng H, Chen J, Lin Z, Xian Y, Huang X, Xie J, Su Z. (2020). Oxyberberine, a novel gut microbiota-mediated metabolite of berberine, possesses superior anti-colitis effect: Impact on intestinal epithelial barrier, gut microbiota profile and TLR4-MyD88-NF-kappaB pathway. Pharmacol Res 152:104603.

Li Q, Zhai W, Jiang Q, Huang R, Liu L, Dai J, Gong W, Du S, Wu Q. (2015). Curcumin-piperine mixtures in self-microemulsifying drug delivery system for ulcerative colitis therapy. Int J Pharm 490:22–31.

Liu C, Jiang Y, Liu G, Guo Z, Jin Q, Long D, Zhou W, Qian K, Zhao H, Liu K. (2022). PPARGC1A affects inflammatory responses in photodynamic therapy (PDT)-treated inflammatory bowel disease (IBD). Biochem Pharmacol 202:115119.

Liu Y, Li BG, Su YH, Zhao RX, Song P, Li H, Cui XH, Gao HM, Zhai RX, Fu XJ, Ren X. (2022). Potential activity of Traditional Chinese Medicine against Ulcerative colitis: A review. J Ethnopharmacol 289:115084.

Liu R, Luo C, Pang Z, Zhang J, Ruan S, Wu M, Wang L, Sun T, Li N, Han L, Shi JJ, Huang YY, Guo WS, Peng SJ, Zhou WH, Gao HL. (2023). Advances of nanoparticles as drug delivery systems for disease diagnosis and treatment. Chin Chem Lett 34:107518.

Ma Y, Yang J, Zhang Y, Zheng C, Liang Z, Lu P, Song F, Wang Y, Zhang J. (2022). Development of a naringenin microemulsion as a prospective ophthalmic delivery system for the treatment of corneal neovascularization: in vitro and in vivo evaluation. Drug Deliv 29:111–27.

Moolakkadath T, Aqil M, Ahad A, Imam SS, Praveen A, Sultana Y, Mujeeb M. (2020). Preparation and optimization of fisetin loaded glycerol based soft nanovesicles by Box-Behnken design. Int J Pharm 578:119125.

Okoshi K, Uekusa Y, Narukawa Y, Kiuchi F. (2021). Solubility enhancement of berberine-baicalin complex by the constituents of Gardenia Fruit. J Nat Med 75:76–83.

Qushawy M, Mortagi Y, Alshaman R, Mokhtar HI, Hisham FA, Alattar A, Liang D, Enan ET, Eltrawy AH, Alamrani ZH, Alshmrani, SA, Zaitone, SA. (2022). Formulation and characterization of O/W nanoemulsions of hemp seed oil for protection from steatohepatitis: analysis of hepatic free fatty acids and oxidation markers. Pharmaceuticals 15:864.

Ravanfar R, Tamaddon AM, Niakousari M, Moein MR. (2016). Preservation of anthocyanins in solid lipid nanoparticles: Optimization of a microemulsion dilution method using the Placket-Burman and Box-Behnken designs. Food Chem 199:573–80.

Shen P, Zhang Z, He Y, Gu C, Zhu K, Li S, Li Y, Lu X, Liu J, Zhang N, Cao Y. (2018). Magnolol treatment attenuates dextran sulphate sodium-induced murine experimental colitis by regulating inflammation and mucosal damage. Life Sci 196:69–76.

Shi H, Zhao X, Gao J, Liu Z, Liu Z, Wang K, Jiang J. (2020). Acid-resistant ROS-responsive hyperbranched polythioether micelles for ulcerative colitis therapy. Chin Chem Lett 31:3102–6.

Singh Y, Meher JG, Raval K, Khan FA, Chaurasia M, Jain NK, Chourasia MK. (2017). Nanoemulsion: Concepts, development and applications in drug delivery. J Control Release 252:28–49.

Subongkot T, Ngawhirunpat T. (2017). Development of a novel microemulsion for oral absorption enhancement of all-trans retinoic acid. Int J Nanomedicine 12:5585–99.

Sun M, Ban W, Ling H, Yu X, He Z, Jiang Q, Sun J. (2022). Emerging nanomedicine and prodrug delivery strategies for the treatment of inflammatory bowel disease. Chin Chem Lett 33:4449–60.

Sun T, Kwong CHT, Gao C, Wei J, Yue L, Zhang J, Ye RD, Wang R. (2020). Amelioration of ulcerative colitis via inflammatory regulation by macrophage-biomimetic nanomedicine. Theranostics 10:10106–19.

Tripathi CB, Parashar P, Arya M, Singh M, Kanoujia J, Kaithwas G, Saraf SA. (2018). QbD-based development of alpha-linolenic acid potentiated nanoemulsion for targeted delivery of doxorubicin in DMBA-induced mammary gland carcinoma: in vitro and in vivo evaluation. Drug Deliv Transl Res 8:1313–34.

Usach I, Alaimo A, Fernandez J, Ambrosini A, Mocini S, Ochiuz L, Peris JE. (2021). Magnolol and honokiol: two natural compounds with similar chemical structure but different physicochemical and stability properties. Pharmaceutics 13:224.

Wang X, Gu H, Zhang H, Xian J, Li J, Fu C, Zhang C, Zhang J. (2021). Oral core-shell nanoparticles embedded in hydrogel microspheres for the efficient site-specific delivery of magnolol and enhanced antiulcerative colitis therapy. ACS Appl Mater Interfaces 13:33948–61.

Wang J, Wang L, Lou GH, Zeng HR, Hu J, Huang QW, Peng W, Yang XB. (2019). Coptidis Rhizoma: a comprehensive review of its traditional uses, botany, phytochemistry, pharmacology and toxicology. Pharm Biol 57:193–225.

Wu Y, Li J, Zhong X, Shi J, Cheng Y, He C, Li J, Zou L, Fu C, Chen M, Zhang J, Gao H. (2022). A pH-sensitive supramolecular nanosystem with chlorin e6 and triptolide co-delivery for chemo-photodynamic combination therapy. Asian J Pharm Sci 17:206–18.

Wu Q, Wei D, Dong L, Liu Y, Ren C, Liu Q, Chen C, Chen J, Pei J. (2019). Variation in the microbial community contributes to the improvement of the main active compounds of Magnolia officinalis Rehd. et Wils in the process of sweating. Chin Med 14:45.

Xie L, Feng S, Zhang X, Zhao W, Feng J, Ma C, Wang R, Song W, Cheng J. (2021). Biological response profiling reveals the functional differences of main alkaloids in rhizoma coptidis. Molecules 26:7389.

Xie Q, Li H, Ma R, Ren M, Li Y, Li J, Chen H, Chen Z, Gong D, Wang J. (2022). Effect of Coptis chinensis franch and Magnolia officinalis on intestinal flora and intestinal barrier in a TNBS-induced ulcerative colitis rats model. Phytomedicine 97:153927.

Yang M, Yang C, Zhang Y, Yan X, Ma Y, Zhang Y, Cao Y, Xu Q, Tu K, Zhang M. (2022). An oral pH-activated "nano-bomb" carrier combined with berberine by regulating gene silencing and gut microbiota for site-specific treatment of ulcerative colitis. Biomater Sci 10:1053–67.

Yen CC, Chen YC, Wu MT, Wang CC, Wu YT. (2018). Nanoemulsion as a strategy for improving the oral bioavailability and anti-inflammatory activity of andrographolide. Int J Nanomedicine 13:669–80.

Zeng F, Wang D, Tian Y, Wang M, Liu R, Xia Z, Huang Y. (2021). Nanoemulsion for improving the oral bioavailability of hesperetin: formulation optimization and absorption mechanism. J Pharm Sci 110:2555–61.

Zhang C, Chen Z, He Y, Xian J, Luo R, Zheng C, Zhang J. (2021). Oral colon-targeting core-shell microparticles loading curcumin for enhanced ulcerative colitis alleviating efficacy. Chin Med 16:92.

Zhang C, Li J, Xiao M, Wang D, Qu Y, Zou L, Zheng C, Zhang J. (2022). Oral colon-targeted mucoadhesive micelles with enzyme-responsive controlled release of curcumin for ulcerative colitis therapy. Chin Chem Lett 33:4924–9.

Zhang C, Wang X, Xiao M, Ma J, Qu Y, Zou L, Zhang J. (2022). Nano-in-micro alginate/chitosan hydrogel via electrospray technology for orally curcumin delivery to effectively alleviate ulcerative colitis. Materials & Design 221:110894.

Zhang FL, Yin XJ, Yan YL, Wu QF. (2022). Pharmacokinetics and pharmacodynamics of Huanglian-Houpo decoction based on berberine hydrochloride and magnolol against H1N1 influenza virus. Eur J Drug Metab Pharmacokinet 47:57–67.

Zhang CL, Zhang S, He WX, Lu JL, Xu YJ, Yang JY, Liu D. (2017). Baicalin may alleviate inflammatory infiltration in dextran sodium sulfate-induced chronic ulcerative colitis via inhibiting IL-33 expression. Life Sci 186:125–32.

Zhang S, Zhao Y, Tan L, Wu S, Zhang Q, Zhao B, Li G. (2022). A novel berberine-glycyrrhizic acid complex formulation enhanced the prevention effect to doxorubicin-induced cardiotoxicity by pharmacokinetic modulation of berberine in rats. Front Pharmacol 13:891829.

Zhao L, Xiao HT, Mu HX, Huang T, Lin ZS, Zhong LLD, Zeng GZ, Fan BM, Lin CY, Bian ZX. (2017). Magnolol, a natural polyphenol, attenuates dextran sulfate sodium-induced colitis in mice. Molecules 22:1218.

Zheng Y, Xu G, Ni Q, Wang Y, Gao Q, Zhang Y. (2022). Microemulsion delivery system improves cellular uptake of genipin and its protective effect against Abeta1-42-induced PC12 cell cytotoxicity. Pharmaceutics 14:617.

Zhong Y, Xiao Q, Li S, Chen L, Long J, Fang W, Yu F, Huang J, Zhao H, Liu D. (2022). Bupi Yichang Pill alleviates dextran sulfate sodium-induced ulcerative colitis in mice by regulating the homeostasis of follicular helper T cells. Phytomedicine 100:154091.

Zhu P, He J, Huang S, Han L, Chang C, Zhang W. (2021). Encapsulation of resveratrol in zein-polyglycerol conjugate stabilized O/W nanoemulsions: Chemical stability, in vitro gastrointestinal digestion, and antioxidant activity. Lwt 149:112049.

Zoya I, He HS, Wang LT, Qi JP, Lu Y, Wu W. (2021). The intragastrointestinal fate of paclitaxel-loaded micelles: Implications on oral drug delivery. Chin Chem Lett 32:1545–9.